ELSEVIER

Journal of Photochemistry and Photobiology A: Chemistry 144 (2001) 119–129

Journal of Photochemistry and Photobiology A:Chemistry

www.elsevier.com/locate/jphotochem

Theoretical quantum chemical study of spironaphthoxazines and their merocyanines Thermal ring-opening reaction and geometric isomerization

Toyokazu Horii*, Yasuo Abe, Ren Nakao

Research Institute for Advanced Science and Technology, Osaka Prefecture University, 1-2 Gakuen-cho, Sakai 599 8570, Japan

Received 9 April 2001; received in revised form 27 June 2001; accepted 29 July 2001

Abstract

We calculate potential energy curves of isomerization in the ground state of spironaphthoxazines (SNO) and their merocyanines (*EZ*, *ZZ*, *EE* and *ZE*) by ab initio methods. We find that in the curves cleavage of the spiro-bond gives firstly cisoid-*ZZ*, followed by the two paths to the *ZZ* isomer by rotation of the central C–N single bond or to the *ZE* isomer by inversion at the nitrogen atom. There is an interconversion path between the resulting *ZZ* and *ZE*, through cisoid-*ZE*. In addition, *ZZ* and *ZE* have paths to *EZ* and *EE*, respectively, by rotation of the C=C bond. We also discuss the photochromic process in terms of the behavior of the specific merocyanines involved in the process.

Keywords: Spironaphthoxazine; Photochromic; Ab initio

1. Introduction

Indoline-spironaphthoxazines and the related indoline-spiropyrans are among the most extensively studied photochromic compounds [1]. UV-irradiation of spironaphthoxazines (SNO), which are colorless induces cleavage of the spiro C–O bond to give a colored open-form isomer called photomerocyanines. Following irradiation, the merocyanine reverts to the spiro-isomer almost completely at room temperature [2]. Several studies using transient spectroscopy have shown the presence of more than one merocyanine isomer [3–7], and NOE experiments using ^{1}H NMR spectroscopy and MO calculations have determined the structure of the most stable isomer [8,9]. In contrast to the spiropyrans, the geometric structures and behavior of the merocyanines of SNO have not been settled because of their thermally unstable character. Moreover, transient spectroscopy studies mainly treat spironaphtho[2,1-b]oxazine (named as β-SNO since it is derived from β-naphthol) and related compounds (Scheme 1). Recently, spironaphtho[1,2-b]oxazine (derived from α-naphthol and named as α-SNO) has been found to show second photochromism at low temperature. This was taken as arised from interconversion of merocyanine isomers [10].

In the present paper, the thermal ring-opening reaction of β- and α-SNO, and the thermal geometric isomerization of their merocyanines are studied using quantum chemistry. Our aim is to clarify the structure and behavior of these species based on their photochromic properties.

2. Computational methods

All molecular orbital calculations were carried out using the GAUSSIAN98 or GAUSSIAN98W set of programs [11]. Minimum energy geometry searches and saddle point searches were carried out at Hartree–Fock (HF) level using the 3-21G* basis sets. The geometries of the stationary points were then reoptimized at the HF and the B3LYP levels using the 6-31G** basis sets. Single point energy evaluations in solution were carried out at the B3LYP/6-31G** level based on gas-phase optimized geometries at the B3LYP/6-31G** level.

3. Results and discussion

3.1. Optimum geometries and energies for spiro-forms and the four stable merocyanine isomers of β- and α-SNO

The structures of four transoid merocyanines (*EZ*, *ZZ*, *EE* and *ZE*) of β- and α-SNO are shown in Scheme 2.

* Corresponding author. Tel.: +81-722-54-9823; fax: +81-722-54-9935.
E-mail address: horii@riast.osakafu-u.ac.jp (T. Horii).

1010-6030/01/$ – see front matter
PII: S1010-6030(01)00541-X

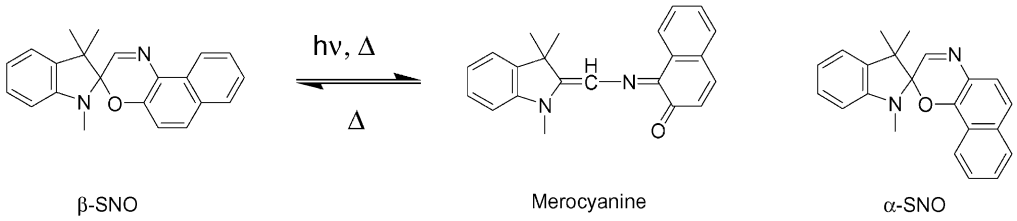

Scheme 1.

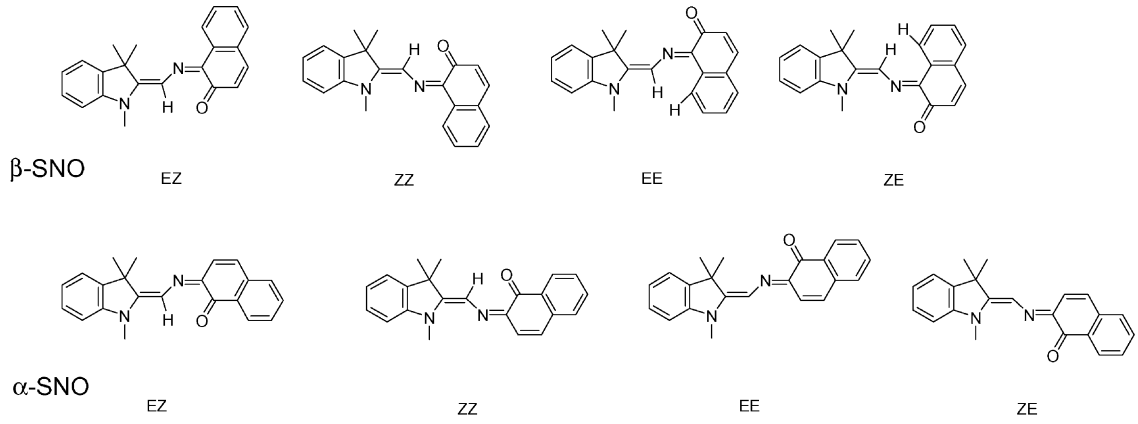

Scheme 2. Structural formulas of merocyanines of β- and α-SNO.

The structures of the spiro-form (named Sp) and the four transoid merocyanines of β- and α-SNO were optimized at the HF/3-21G* levels. All transoids were planar structures. However, harmonic vibration analysis revealed that the planar structures for *EE* and *ZE* of β-SNO were transition states rather than minimum energy geometries.

Reoptimization was performed at the HF/6-31G** and B3LYP/6-31G** levels for the planar structures; the parts of optimized structures at the HF/6-31G** levels are shown in Table 1. Only *EE* and *ZE* of β-SNO exhibited nonplanar minimum energy geometries; these have planar chirality. The corresponding naphthoquinoneimine rings are twisted and deformed into the third dimension.

These nonplanar structures exhibit reduced repulsion between the central hydrogen and the naphthalene hydrogen. The planar *EE* and *ZE* structures were found to be the transition state for interconversion between the chiral nonplanar isomers. In the planar *EE* and *ZE* structures of β-SNO, the central hydrogen and the closest hydrogen of the naphthalene ring lie close together ($H_{C}{=}_{C} \cdots H_{naphtho}$, 1.77 Å) despite the increased bond angle of C–N=C (135.2°). In the nonplanar structure, H–H repulsion is reduced by the twist and by deformation ($H_{C}{=}_{C} \cdots H_{naphtho}$, 2.06 Å). The *EZ* and *ZZ* forms of β- and α-SNO have similar separations (2.11–2.16 Å) of the central hydrogen and the carbonyl oxygen suggesting an electrostatic interaction.

The relative energies of the four merocyanines for Sp are shown in the first five rows of Table 2. *EZ* and *ZZ* are more stable than *EE* and *ZE* in β-SNO because of destabilization as a result of the nonplanar structure of *EE* and *ZE*. Also, the relative energies of merocyanines are lower based on B3LYP than HF; for *EZ*, the most stable merocyanine isomer, the value is only 2.0 kJ mol^{-1} in α-SNO compared with 12.8 kJ mol^{-1} in β-SNO. Values for α-SNO are reduced further in solutions to negative values causing instability.

Table 1
Optimized structures of the merocyanine isomers (interatomic distances; bond angles, torsion angles in Å and °, respectively) at the HF/6-31G** level

	α-SNO				β-SNO			
	EZ	*ZZ*	*EE*	*ZE*	*EZ*	*ZZ*	*EE* (planar)	*ZE* (planar)
$H_{C}{=}_{C} \cdots O(=C)$	2.155	2.156			2.113	2.105		
$H_{C}{=}_{C} \cdots H_{naphtho}$			2.101	2.100			2.056 (1.772)	2.060 (1.768)
C=C–N	118.6	121.7	118.5	121.5	119.4	122.7	118.3 (117.7)	122.1 (120.8)
C–N=C	127.1	127.1	126.3	126.3	127.2	126.8	129.1 (135.2)	129.2 (135.2)
C=C–N=C	180.0	180.0	180.0	180.0	180.0	180.0	177.6 (180.0)	177.3 (180.0)
N=C–C=O	0.0	0.0	0.0	0.0	0.0	0.0	25.6 (0.0)	25.1 (0.0)

Table 2
Relative energies (kJ mol^{-1}) and dipole moments (Debye) of stationary points of α- and β-SNO in gas phase and in solutions

	Gas phase					In cyclohexane	In acetone	In ethanol
	HF/3-21G*	HF/6-31G**		B3LYP/6-31G**		PCM-B3LYP/6-31G**[a]	PCM-B3LYP/6-31G**	PCM-B3LYP/6-31G**
	Energies	Energies	Dipole moments	Energies	Dipole moments	Energies	Energies	Energies
α-SNO								
Sp	0.00	0.00	1.0911	0.00	0.8328	0.00	0.00	0.00
EZ	46.33	40.96	1.2397	2.00	3.6445	−0.32	−3.77	−9.04
ZZ	62.03	48.55	2.1372	8.53	4.1398	5.97	1.89	−2.85
EE	71.98	50.79	4.3929	19.75	5.4744	15.67	8.52	3.12
ZE	78.48	55.81	3.2251	21.72	4.3100	18.58	13.27	8.02
Cisoid-*ZZ*	129.24	105.76	2.3542	57.59	3.3383	55.72	52.08	48.38
Cisoid-*ZE*	131.30	99.13	4.2585	78.41	4.8435	73.08	64.48	58.17
TS1	192.43	167.86	15.1054	132.88	13.1318	116.64	94.60	78.96
TS2	238.35	204.59	14.1730	171.30	13.2685	152.90	126.46	108.88
TS3	187.34	173.89	4.2618	129.24	5.2767	124.10	116.05	108.81
TS4	177.69	169.47	1.6154	118.60	3.1426	116.81	113.77	110.85
TS5	141.00	108.87	3.5479	98.53	4.3513	96.62	93.51	86.83
TS6	134.82	99.95	4.2475	93.33	4.1525	89.51	83.32	74.54
TS7	140.84	132.17	7.4155	72.33	5.2373	69.18	63.62	57.85
β-SNO								
Sp	0.00	0.00	0.8726	0.00	0.6336	0.00	0.00	0.00
EZ	65.29	50.90	1.7387	12.79	3.6496	9.66	5.04	2.81
ZZ	74.78	58.89	2.7674	19.37	4.2718	16.43	11.59	9.27
EE	103.75	78.12	5.2143	48.56	5.6921	44.01	36.88	31.83
ZE	104.45	81.21	4.1337	46.08	4.4286	42.16	35.88	33.53
Cisoid-*ZZ*	136.06	110.71	2.8071	63.96	3.1011	61.97	58.28	55.26
Cisoid-*ZE*	166.57			107.41	5.1455	101.53	92.56	84.32
TS1	204.51	176.64	13.7036	140.01	11.8716	124.68	103.93	91.24
TS2	259.78	226.82	11.6216	188.53	9.9461	174.85	154.8	140.27
TS3	201.79	182.97	4.4326	141.71	5.2459	136.50	128.78	123.06
TS4	187.19	172.63	2.1421	123.63	3.1868	121.26	117.65	117.62
TS5	146.09	113.97	3.6657	104.03	4.6077	102.24	99.60	96.14
TS6	167.43			117.94	4.4826	114.01	107.90	102.33
TS7	150.88	117.42	6.9023	75.90	4.8926	72.92	67.69	61.03
TS_{EE}[b]	103.84	87.35	4.8535	52.42	5.5682	70.00	64.75	
TS_{ZE}[b]	112.28	92.19	3.6788	53.42	4.3594	49.81	43.62	

[a] Based on gas-phase geometries at the B3LYP/6-31G**.
[b] Planar *EE* or *ZE*.

3.2. Isomeric reactions of the four merocyanine isomers and opening the ring of the spiro-form

Interconversion between *EZ* and *ZZ*, or between *EE* and *ZE*, takes place by rotation around the C=C bond. By contrast interconversion between *EZ* and *EE*, or between *ZZ* and *ZE*, involves two paths: (1) rotation of the N=C bonds, and (2) through the cisoid isomer produced by inversion in the –N= atom or rotation of the central C–N bond. Also, the thermal ring-opening reaction of Sp should pass through the cisoid-like structure to give the stable transoids.

3.2.1. α-Spironaphthoxazine

3.2.1.1. Rotation around C=C bond. The search for transition states in conversions between *EZ* and *ZZ*, and

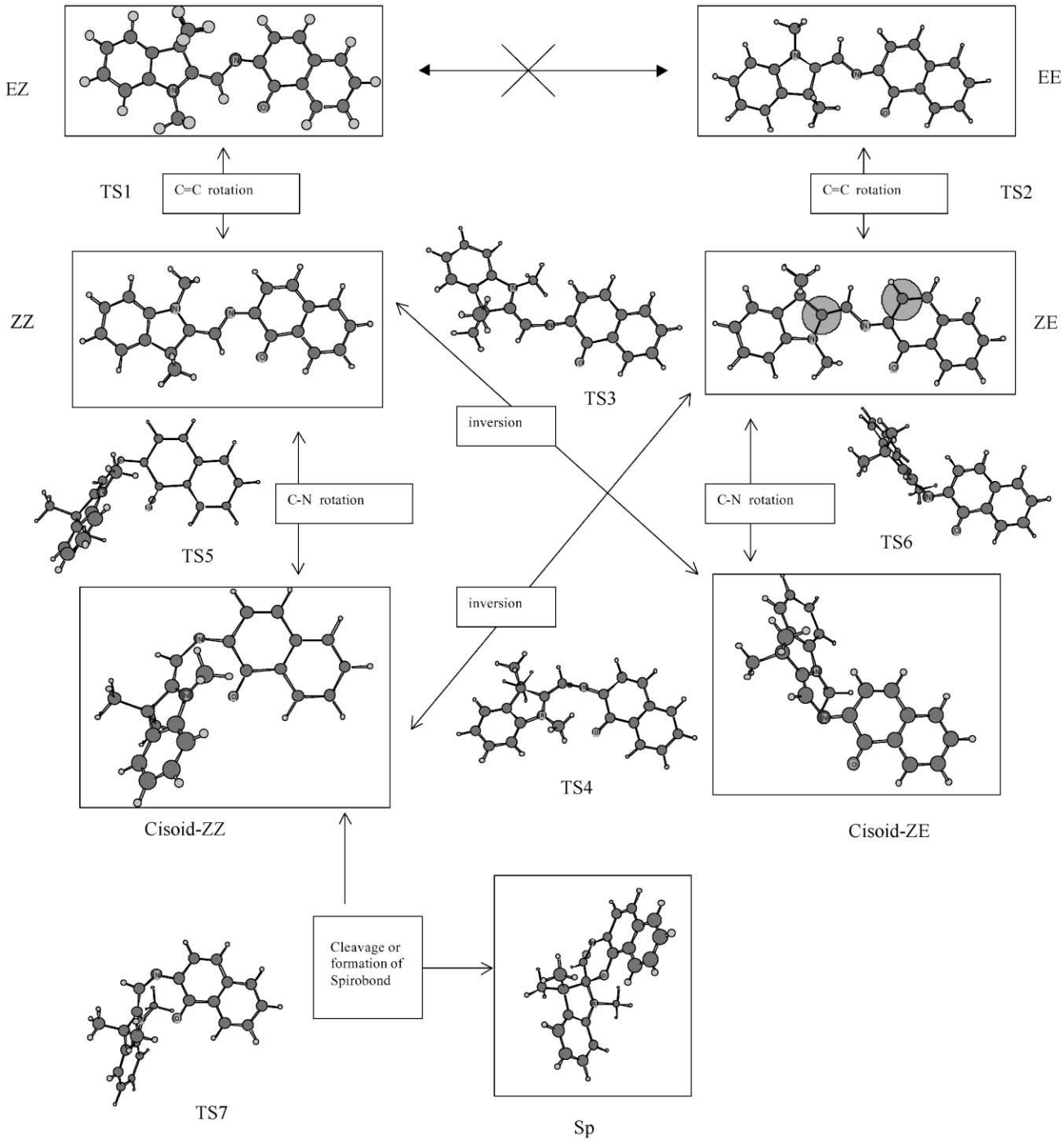

Scheme 3. Isomerization of α-SNO (HF/3-21G*).

between *EE* and *ZE*, revealed the transition states TS1 and TS2 having structures rotated by about 90° around the C=C bond (Scheme 3). Calculations were performed with the HF/3-21G* and then with the HF/6-31G** and the B3LYP/6-31G** levels (Table 2).

3.2.1.2. Isomerization about the N=C bond and the ring-opening reaction. We have investigated the geometry of the isomerization reaction between *ZZ* and *ZE*. First, to investigate the possibility of rotation around the N=C bond, constrained optimization was carried out at a fixed value of the torsion angle around the N=C bond at the HF/3-21G* level. Structures could not be obtained for torsion angles exceeding 60°.

Next, the reaction path for inversion at the N atom of the N=C bond of *ZZ* or *ZE* was sought. This process involves searching over the potential energy surface so that constrained optimization at a fixed value of the C–N=C bond angle was carried out at the HF/3-21G* level. A saddle point and a local minimum were found for each; the results of these calculations are shown in Fig. 1. Also, calculations on the rotation a round the central C–N single bond were carried out by the same method at a fixed value of the torsion angle; a saddle point and the local minimum as a shallow basin were obtained in each case. The local minimum by inversion from *ZZ* is equal to that by rotation from *ZE* (named cisoid-*ZE*). Also, the local minimum by inversion from *ZE* is equal to that by rotation from *ZZ* named cisoid-*ZZ*. Accordingly, there are two possible paths of interconversion between *ZZ* and *ZE* initiated either by inversion or rotation.

The geometry of the ring-opening reaction was then investigated to find a saddle point and a local minimum point based on searching over the potential energy surface. The local minimum point was found to be equal to cisoid-*ZZ* (see Fig. 1). These local minima, cisoid-*ZE* and cisoid-*ZZ* have nonplanar pseudo-cisoid structures, and the nitrogen atom of the indoline ring has a low pyramidal structure.

These two local minima and five saddle points were optimized at the HF/3-21G* level, and the transition states TS3, TS4, TS5, TS6 and TS7 were confirmed to be connected to the reactants and the products using intrinsic reaction coordinate (IRC) methods. These structures are shown in Scheme 3 and Table 3 and the energy diagram in Fig. 2.

No similar path of interconversion between *EZ* and *EE* could be found so that inversion or rotation in *EZ* and *EE* cannot proceed to give nonplanar pseudo-cisoid isomers. The reason is taken to be steric hindrance by either of the two methyl groups deviating up and down from the plane of the indoline ring. In cisoid-*ZZ* and cisoid-*ZE*, the pyramidal structure of the nitrogen atom of the indoline ring is able to prevent steric hindrance by the methyl groups at the N atom.

In summary, the first step by which *ZZ* transforms to *ZE* starts by inversion at the N atom with only a small change in torsion angle around the central C–N single bond to TS3, until the three atoms C–N=C (bond angle, 170°) are aligned almost linearly. Inversion continues to give

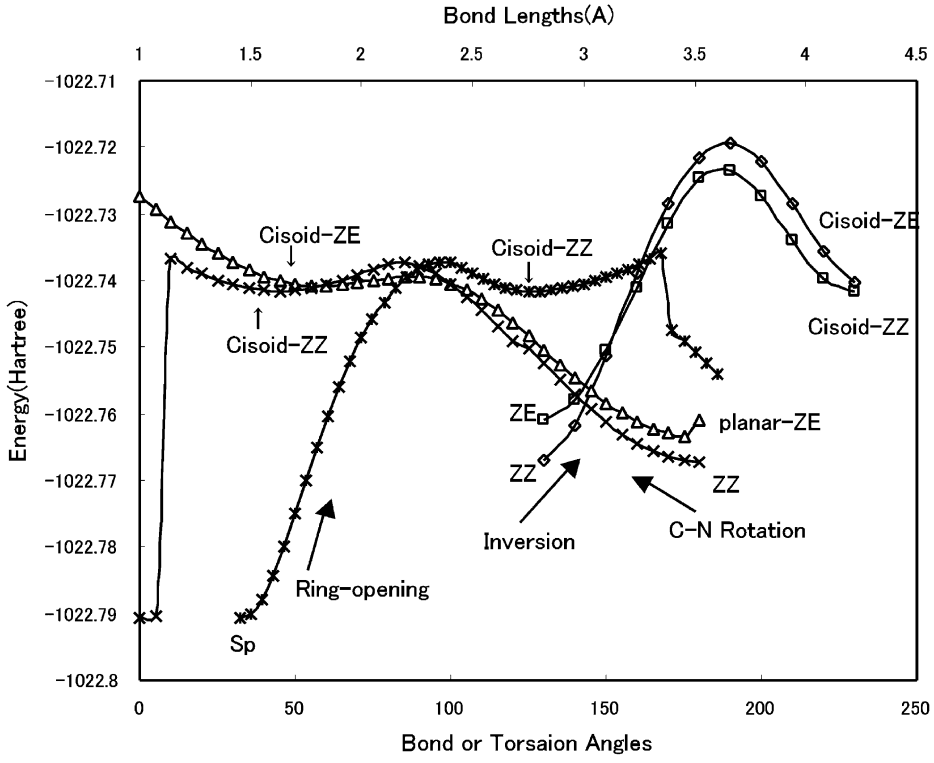

Fig. 1. Potential energy surfaces of *ZZ–ZE* isomerization and ring-opening reaction of α-SNO (HF/3-21G*).

Table 3
Optimized structures of the spiro- and cisoid isomers and the transition states (torsion angles, interatomic distances and bond angles)

	HF/3-21G*		HF/6-31G**		B3LYP/6-31G**	
	∠C–N–C–C (°)	C···O (Å)	∠C–N–C–C (°)	C···O (Å)	∠C–N–C–C (°)	C···O (Å)
α-SNO						
Sp	1.8	1.461	1.7	1.421	2.0	1.463
TS7	17.8	2.378	12.9	2.351	17.0	2.193
Cisoid-*ZZ*	44.3	2.780	57.8	2.919	35.8	2.711
TS5	82.5	3.171	74.5	3.207	93.8	3.314
TS4	58.4	171.0[a]	57.4	169.9[a]	75.9	171.3[a]
Cisoid-*ZE*	58.1		67.7		50.9	
TS6	87.5		86.1		94.4	
TS3	48.1	169.9[a]	55.3	170.8[a]	54.4	169.7[a]
β-SNO						
Sp	1.6	1.455	1.7	1.422	2.0	1.462
TS7	19.8	2.344	14.6	2.341	19.6	2.203
Cisoid-*ZZ*	47.6	2.781	62.7	2.913	37.6	2.689
TS5	81.6	3.148	68.9	3.119	93.1	3.303
TS4	61.8	167.8[a]	74.7	172.2[a]	76.4	171.1[a]
Cisoid-*ZE*	60.9		–	–	55.4	
TS6	85.7		–	–	97.1	
TS3	68.4	172.1[a]	74.7	172.3[a]	66.9	171.0[a]

[a] C–N–C bond angles (°).

nonplanar cisoid-*ZE* (torsion angle, 58.1°). The second step is a rotation about the C–N single bond resulting in planar *ZE*. Inversion of *ZE* to *ZZ* progresses similarly over TS4 via nonplanar cisoid-*ZZ*. TS3 and TS4 are transition states with a near-sp-hybridized bond of the nitrogen atom.

Cisoid-*ZZ* is also the first product in the ring-opening reaction proceeding further to *ZZ* over TS5 by rotation of the C–N single bond, or to *ZE* over TS4 by inversion at the N atom. The former reaction should take place over the latter because the energy of TS5 is lower than that of TS4.

We further carried out reoptimization at the HF/6-31G** and B3LYP/6-31G** levels for these seven stationary points. Results are shown in Table 2 and the energy diagrams in Fig. 3. The difference between the two methods causes some changes in the optimized structures, especially of cisoid isomers and the relative transition states (Table 3). Then, it

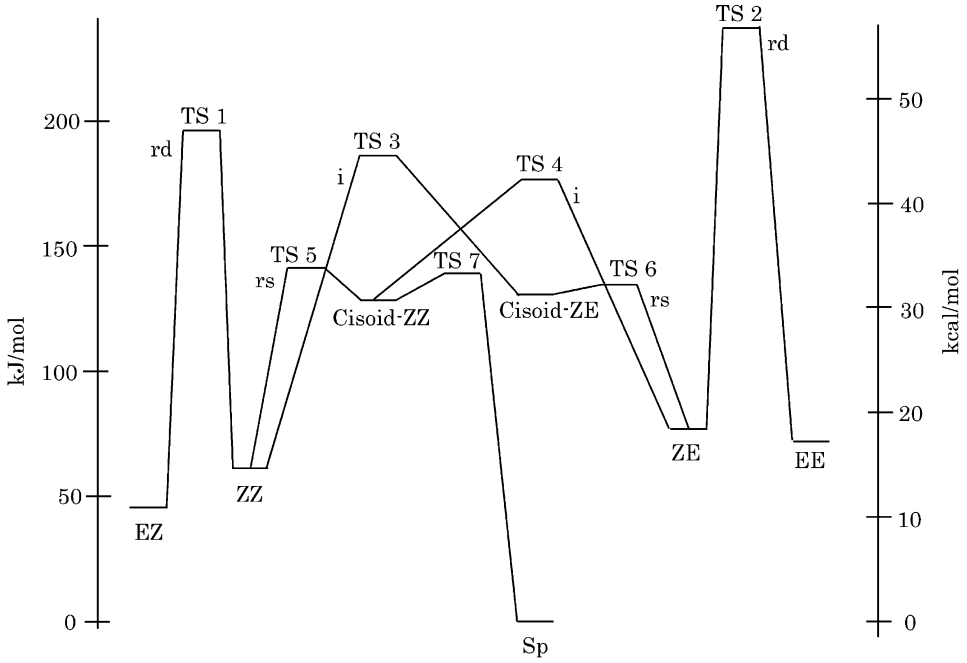

Fig. 2. Energy diagrams of α-SNO in the gas phase at the HF/3-21G* level (rd, rotation about C=C bond; i, inversion at N atom; rs, rotation about C–N bond).

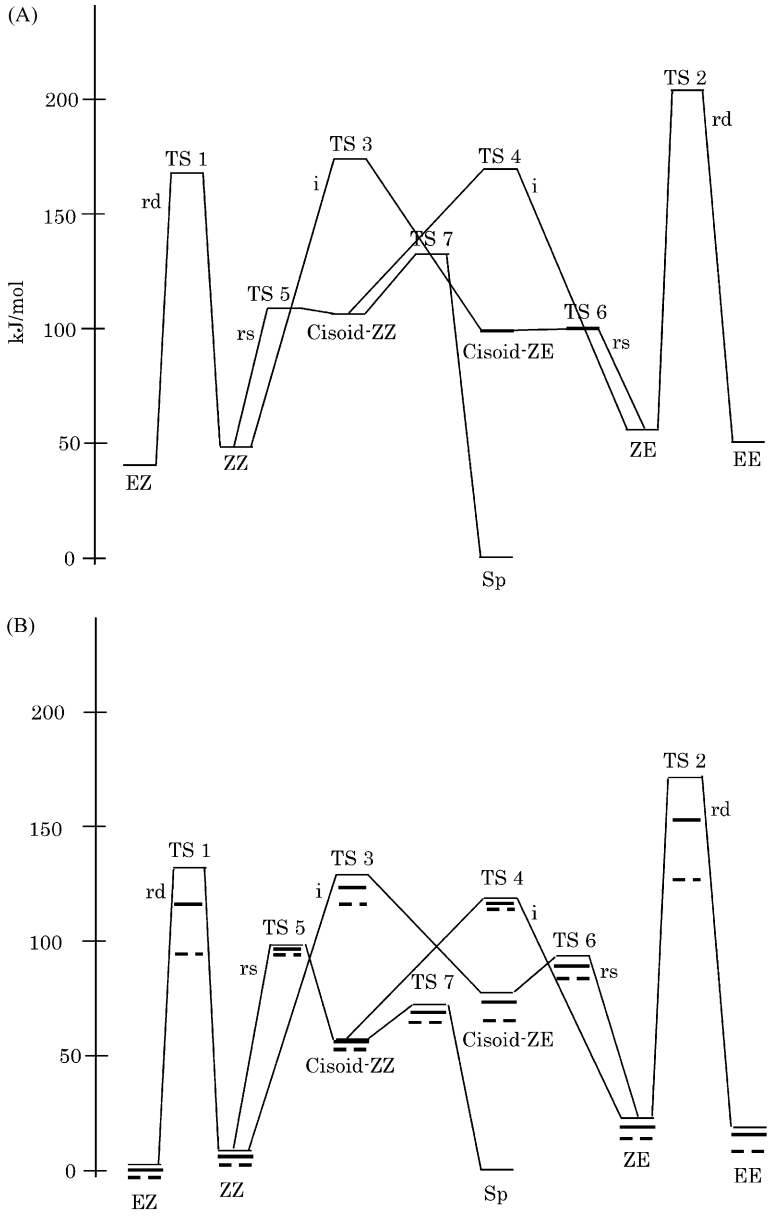

Fig. 3. Energy diagrams of α-SNO in the gas phase: (A) at the HF/6-31G** level, and (B) at the B3LYP/6-31G** level (rd, rotation about C=C bond; i, inversion at N atom; rs, rotation about C–N bond). Bold and broken lines showed energies at the PCM-B3LYP**/6-31G**//B3LYP/6-31G** in cyclohexane and ethanol, respectively.

was reconfirmed using IRC method at both the levels that TS5 was connected to *ZZ* and cisoid-*ZZ*, and TS7 to Sp and cisoid-*ZZ*.

Comparison of the results of HF and B3LYP shows that the inclusion of electron correlation effects (in B3LYP) deepens the basins of cisoid-*ZZ* and cisoid-*ZE* and favors the ring-closure reaction of cisoid-*ZZ* over C–N rotation to *ZZ* (TS7 < TS5). The order (TS7 < TS5) is unchanged also in single point energy evaluations at the B3LYP/6-31G** level based on optimized geometries at the HF/6-31G** level. Consequently, the reversion of the heights results not from the change of the optimized structures but from the electron correlation effects.

3.2.2. β-Spironaphthoxazine

We also made calculations for β-SNO at the 3-21G* level, using the same methods as for α-SNO, and found two local minimum points, cisoid-*ZZ* and cisoid-*ZE* and seven transition states TS1, TS2, TS3, TS4, TS5, TS6 and TS7. However, the basin of cisoid-*ZE* was so shallow that the energy of TS6 was higher by only 0.86 kJ mol^{-1} than that of cisoid-*ZE*. Reoptimization at the HF/6-31G** level showed that cisoid-*ZE* was no longer a local minimum point. At the B3LYP/6-31G** level, cisoid-*ZE* and TS6 were again a minimum point and a transition state, respectively. These results are shown in Table 2 and the energy diagrams in Fig. 4.

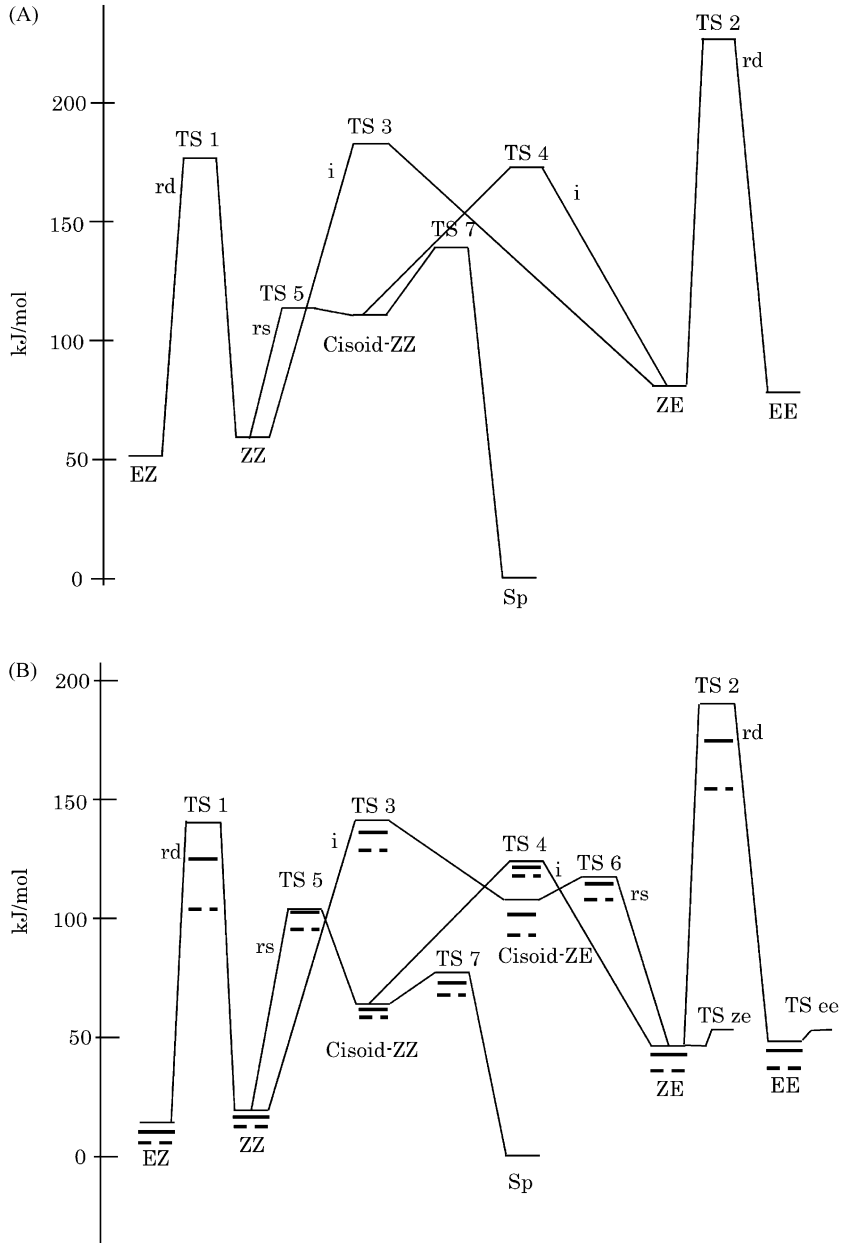

Fig. 4. Energy diagrams of β-SNO in the gas phase: (A) at the HF/6-31G** level, and (B) at the B3LYP/6-31G** level (rd, rotation about C=C bond; i, inversion at N atom; rs, rotation about C–N bond). Bold and broken lines showed energies at the PCM-B3LYP**/6-31G**//B3LYP/6-31G** in cyclohexane and ethanol, respectively.

3.3. Dipole moments and results in liquid phase

Dipole moments are shown in Table 2. The moments of TS1 and TS2 in α-SNO are much larger than the others at the HF/6-31G** and B3LYP/6-31G** levels. Similar results are obtained for β-SNO. Based on gas-phase optimized geometries at the B3LYP/6-31G** level, relative energies in cyclohexane, acetone and ethanol from PCM-B3LYP/6-31G** calculations are shown in Table 2, and the energy diagrams in cyclohexane and ethanol are shown in Figs. 3(B) and 4(B). Bold and broken lines show energies in cyclohexane and ethanol, respectively. As predicted from the dipole moments, the relative energies of TS1 and TS2 are much lower in polar than in nonpolar solvents. For example, in α-SNO the difference in relative energies in ethanol and cyclohexane are 38 kJ mol^{-1} for TS1 and 44 kJ mol^{-1} for TS2, but the rest are all less than 16 kJ mol^{-1}.

3.4. Thermal behaviors of photomerocyanine and calculated energy diagrams

Generally, the absorption spectrum of SNO in solutions has a peak near 320 nm due to the spiro-form (Sp). The spectrum contains a second weak band at 580–610 nm. This

band is attributed to the *trans*-merocyanine isomer (denoted transoid) which is in equilibrium with the Sp form.

$$\text{Sp} \rightleftharpoons \text{transoid}$$

Dissociation of the C–O spiro-bond of Sp should give rise to the cisoid-*ZZ* isomer, and subsequently to the stable transoids. The cisoid-*ZZ* isomer, having a structure similar to the initial spiro-form but with a dissociated C–O spiro-bond is reported to be the initial product of photocoloration of spirobenzopyran [12]. However, existence of the cisoid-*ZZ* in SNO is unclear. The transoid concentration in equilibrium with Sp can be greatly increased by irradiation at $\lambda <$ 400 nm. The quantum yields of photocoloration of β-SNO are 0.41 in methylcyclohexane and 0.32 in ethanol [16]. The ring opening of β-SNO occurs in the S_1 state [13,14]. In a femtosecond (fs) transient spectroscopic study, the S_1 state with lifetime of 700 fs relaxes to a transition state and within the following 470 fs results in the merocyanines [6].

Regarding the distribution of the four possible transoids, only *EZ* and small amounts of *ZZ* were detected in NOE experiments using ^{1}H NMR spectroscopy at low temperature [8,9]. However, these two experiments were carried out exclusively in polar solvents (methanol and acetonitrile), since they are difficult to perform in nonpolar solvents such as hydrocarbons. The distribution of *EZ* and *ZZ* might be different in nonpolar solvents.

We now consider the thermal behavior of photomerocyanines based on the calculated results. We begin with β-SNO for which much more experimental reports exist than for α-SNO. The potential energy surface of the ground state (S_0) from the Sp form to merocyanines, based on the energies in cyclohexane in Fig. 4(B), is illustrated in Scheme 4(A) with a hypothetical surface of the excited singlet state (S_1).

There are two possible calculated potential energy surfaces of the S_0 state through TS5 and *ZZ* to *EZ*, and through TS4, *ZE* and cisoid-*ZE* to *EZ*. In the thermal reaction, the first path is preferred (TS5 < TS4). However, in photocoloration, the potential energy surface of S_1 is considered to pass above the latter surface of S_0, as illustrated in Scheme 4(A), because of the possibility of formation of *ZE* as described later. We considered the three cases with respect to the products by relaxations of the S_1 state of Sp to merocyanines which should occur: (i) near TS4 to cisoid-*ZZ* and *ZE*; (ii) near TS3 to *ZZ* and cisoid-*ZE*; (iii) near TS1 to *EZ* and *ZZ*.

The cisoid-*ZZ* have an energy minimum in a basin surrounded by TS7, TS5 and TS4. However, TS7 is lower than TS5 or TS4, so that the barrier of reformation of the spiro-bond is lower than that of the rotation or inversion to more stable transoid isomers at the B3LYP/6-31G** level. It follows that the formation of cisoid-*ZZ* cannot lead to rotation or inversion to more stable transoid isomers.

If the first products on irradiation of Sp are *ZE* and/or *ZZ*, they could not isomerize rapidly to the most stable *EZ* because the height of TS1 is greater than that of TS4 or TS5. On the other hand, the ring opening of β-SNO and distribution of isomers are both very fast, and the absorption spectra of colored SNOs are independent of temperature [2,5,15]. It is, therefore, more likely that *EZ* arises not by thermodynamic isomerization of recently produced *ZZ* or *ZE*, but directly from the S_1 state [7]. Utilization ratios of these pathways of relaxation of the S_1 state might depend on solvents. Path (iii) is a major one in polar solvents accompanied in nonpolar solvents by path (ii). The back reaction to Sp by path (i) should cause a lower quantum yield of photocoloration than 1.0 [16].

Several transit spectroscopic studies of β-SNO show the thermodynamic behaviors of the photomerocyanines [3–7]. Photocoloration of β-SNO at room temperature occurs in a two-step process with a major component taking place within 10 ns, and a very short-life minor second one with $t_{1/2} < 1\,\mu$s [7]. This minor component is considered not to be a transoid but the relatively unstable cisoid-*ZE*, because the barriers for interconversion between the transoids are higher than for ring closure of *ZZ* or *ZE*.

The relaxation kinetics of the merocyanine form is known to follow first-order decay at various temperatures [2,16]. In addition, two separate steps begin from two distinct photoisomers and lead to the ring closure, i.e. major and minor components. The relevant activation energies E_1 and E_2 are, respectively, 65 and 78 kJ mol^{-1} in methylcyclohexane, and 62 and 69 kJ mol^{-1} in toluene (see Table 4). These two isomers can be taken to correspond *ZZ* and minor *ZE* in Scheme 4(A). The calculated activation energies of *ZZ* and *ZE* for overcoming TS5 (E_1) and TS4 (E_2) to Sp are 86–87 and 79–84 kJ mol^{-1} in solution, respectively. These values are somewhat larger than the observed values but are close to each other. On the other hand, the minor component is not detectable in polar solvents as ethanol and acetone. An explanation is that the pathway of the S_1 to the S_0 cannot occur via path (ii) in polar solvents but rather through path (iii). This might be related to the fact that the barrier of TS1 is much lower in polar solvents (Fig. 4(B)).

Upon excitation of the merocyanine at 530 nm below −10°C, a bleaching over the vis-spectrum was observed and a weak transient absorption below 400 nm. The kinetics of bleaching recovery and absorption decay were of first order and practically identical. The activation energies (E_3) of the bleaching recovery are in the range 21–28 kJ mol^{-1} in various solvents. The excited merocyanines should be *EZ* and *ZZ*. The possible bleaching intermediate is cisoid-*ZE* or cisoid-*ZZ* by the excitation of *ZZ*, but a transient absorption below 400 nm should be due to cisoid-*ZE* because cisoid-*ZZ* cannot recover merocyanines. As shown in Scheme 4(A), bleaching recovery could

$$ZZ \xrightarrow{h\nu} \text{cisoid-}ZE \xrightarrow{\Delta} ZE$$

correspond to the path by which cisoid-*ZE* overcomes TS6 to *ZE*. The recovered product should be *ZE* rather than *ZZ*, but the results cannot distinguish. The activation energies are 18 kJ mol^{-1} in ethanol and 12 kJ mol^{-1} in cyclohexane; these values are somewhat smaller than the experimental

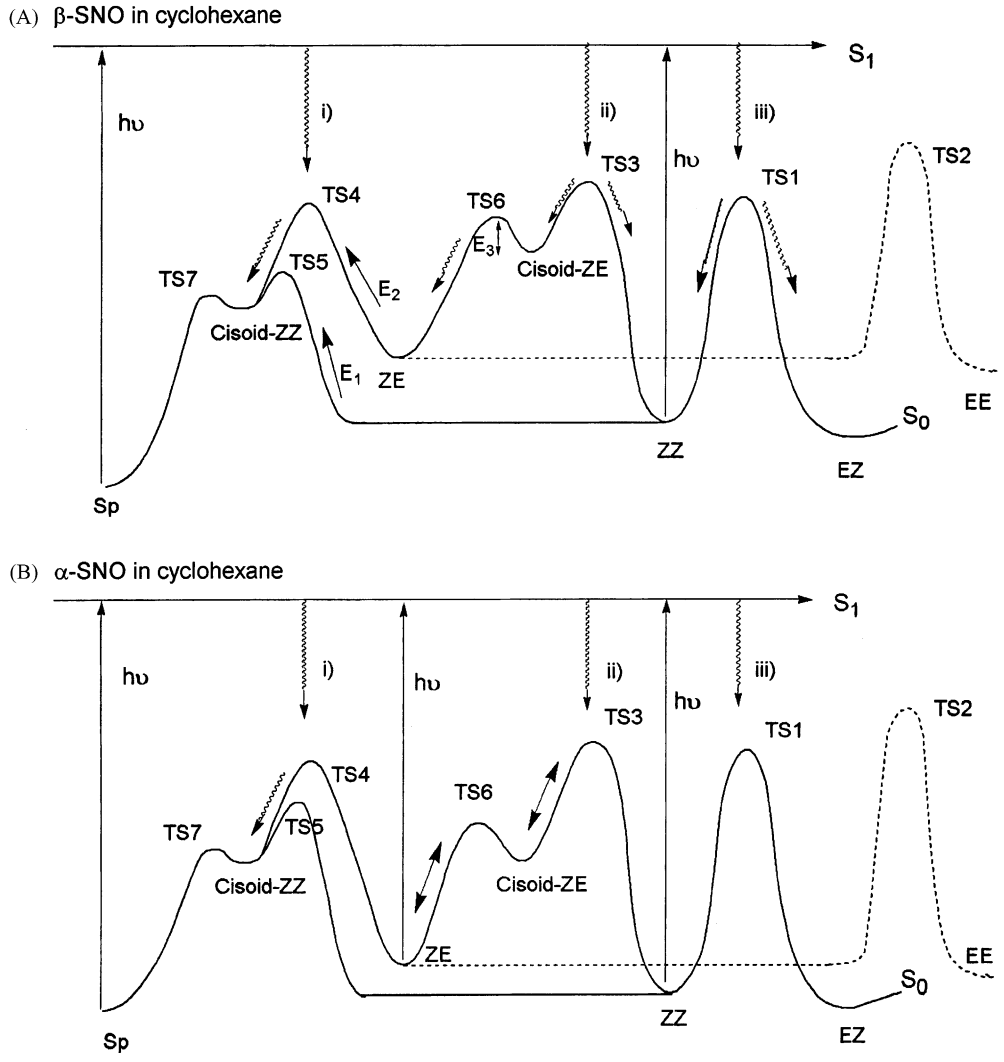

Scheme 4.

results. In polar solvents, the bleaching and recovery are much smaller because the main merocyanine isomer is *EZ* in polar solvents. If irradiation of *ZZ* cannot drive directly to Sp, photodecoloration is considered to occur by excitation of *ZE*. Photodecoloration to Sp at low temperature is taken to occur by irradiation of *ZE* that has accumulated by longtime irradiation. Such photoisomerizations between transoids explain the low quantum yields in the photodecoloration of merocyanines [10].

A similar potential energy curve for α-SNO in cyclohexane, based on Fig. 3(B), is shown in Scheme 4(B). Here, the relative potential energies of *ZE*, *EE* and cisoid-*ZE* of α-SNO are rather lower than those of β-SNO. No transient spectroscopic studies have been made of α-SNO. However, in studies of the spectra of UV-irradiated solutions of α-SNO at low temperature, the photomerocyanines themselves exhibited thermally reversible photochromism [10]. Specifically, the spectra of the merocyanines in hexane at 183 K showed

Table 4
Activation energies (kJ mol^{-1}) in the reactions of the merocyanines of β-SNO in solutions

	Experimental values[a]			Calculated values	
	Methylcyclohexane	Toluene	Ethanol	Cyclohexane	Ethanol
E_1 (kJ mol^{-1})	65, 71[b]	62	85, 81[b]	86	87
E_2 (kJ mol^{-1})	78	69		79	84
E_3 (kJ mol^{-1})	25	21		12	18

[a] From Ref. [7] unless indicated.
[b] From Ref. [16].

four absorption maxima (615, 579, 545 and 510 nm). Irradiation with light at >600 nm reduced the two peaks of the longest wavelength and increased the two peaks of the shortest wavelength. After 30 min, the photostationary state was reached. When irradiation was stopped, the spectrum returned gradually to the pre-irradiated spectrum taking about 2 h. This second photochromism suggests the existence of a metastable isomer that permits interconversion between the geometric isomers of the merocyanine even at low temperatures. The possible metastable isomer is cisoid-*ZE* and *ZE*. Irradiation of *ZZ* increases cisoid-*ZE* and *ZE*, and stopping the irradiation causes the reverse reaction. Additionally, irradiation of the merocyanine isomers with light of >500 nm results in photodecoloration of *ZE* to Sp at very low quantum yield.

$$ZZ \underset{\Delta}{\overset{h\nu}{\rightleftharpoons}} \text{cisoid-}ZE \underset{\Delta}{\overset{\Delta}{\rightleftharpoons}} ZE \xrightarrow{h\nu} \text{Sp}$$

4. Conclusion

We have calculated the potential energy curves of the reactions in the ground state of SNO and the associated merocyanines. In the curves, cleavage of the spiro-bond first gives rise to cisoid-*ZZ*. Then two possible paths arise to *ZZ* by C–N rotation and to *ZE* by N inversion. A path exists for interconversion between the resulting *ZZ* and *ZE* through cisoid-*ZE*. In addition, *ZZ* and *ZE* have paths to *EZ* and *EE*, respectively, by rotation of the C=C bond. On the basis of the potential energy curves, the structures and behaviors of the relevant photomerocyanine isomers and especially the role of two metastable isomers, cisoid-*ZE* and cisoid-*ZZ*, have been elucidated.

References

[1] R. Guglielmetti, N.Y.C. Chu, in: H. Dürr, H. Bouas-Laurent (Eds.), Photochromism: Molecules and Systems, Elsevier, Amsterdam, 1990 (Chapters 8 and 10) and references cited therein.
[2] N.Y.C. Chu, Can. J. Chem. 61 (1983) 300.
[3] S. Schneider, Z. Phys. Chem. Neue Fol. 154 (1987) 91.
[4] A. Kellmann, F. Tfibel, R. Dubest, P. Levoir, J. Aubard, E. Pottier, R. Guglielmetti, J. Photochem. Photobiol. A 49 (1989) 63.
[5] S. Aramaki, G.H. Atkinson, Chem. Phys. Lett. 170 (1990) 181.
[6] N. Tamai, H. Masuhara, Chem. Phys. Lett. 191 (1992) 189.
[7] A.K. Chibisov, H. Görner, J. Phys. Chem. A 103 (1999) 5211 and references cited therein.
[8] S. Nakamura, K. Uchida, A. Muraoka, M. Irie, J. Org. Chem. 58 (1993) 5543.
[9] S. Delbaere, C. Bochu, N. Azaroual, G. Buntinx, G. Vermeersch, J. Chem. Soc., Perkin Trans. 2 (1997) 1499.
[10] T. Horii, Y. Miyake, R. Nakao, Y. Abe, Chem. Lett. 1997 (1997) 655.
[11] M.J. Frisch, G.W. Trucks, H.B. Schlegel, G.E. Scuseria, M.A. Robb, J.R. Cheeseman, V.G. Zakrzewski, J.A. Montgomery Jr., R.E. Stratmann, J.C. Burant, S. Dapprich, J.M. Millam, A.D. Daniels, K.N. Kudin, M.C. Strain, O. Farkas, J. Tomasi, V. Barone, M. Cossi, R. Cammi, B. Mennucci, C. Pomelli, C. Adamo, S. Clifford, J. Ochterski, G.A. Petersson, P.Y. Ayala, Q. Cui, K. Morokuma, D.K. Malick, A.D. Rabuck, K. Raghavachari, J.B. Foresman, J. Cioslowski, J.V. Ortiz, B.B. Stefanov, G. Liu, A. Liashenko, P. Piskorz, I. Komaromi, R. Gomperts, R.L. Martin, D.J. Fox, T. Keith, M.A. Al-Laham, C.Y. Peng, A. Nanayakkara, C. Gonzalez, M. Challacombe, P.M.W. Gill, B. Johnson, W. Chen, M.W. Wong, J.L. Andres, C. Gonzalez, M. Head-Gordon, E.S. Replogle, J.A. Pople, GAUSSIAN'98, Revision A.6, Gaussian, Inc., Pittsburgh, PA, 1998.
[12] A.K. Chibisov, H. Görner, J. Phys. Chem. A 101 (1997) 4305.
[13] F. Willkinson, D.R. Worrall, J. Hobley, L. Jansen, S.L. Williams, A.J. Langley, P. Matousek, J. Chem. Soc., Faraday Trans. 92 (1996) 1331.
[14] A. Kellmann, F. Tfibel, R. Guglielmetti, J. Photochem. Photobiol. A 91 (1995) 131.
[15] V.G. Luchina, I.Yu. Sychev, A.I. Shienok, N.L. Zaichenko, V.S. Marevtsev, J. Photochem. Photobiol. A 93 (1996) 173.
[16] G. Favaro, F. Malatesta, U. Mazzukato, G. Ottavi, A. Romani, J. Photochem. Photobiol. A 87 (1995) 235.